CYBERNETICS AND PHYSICS, VOL. 7, NO. 2, 2018 , 49–56

PREACCELERATION OF THE MULTICHARGED IONS WITH THE DIFFERENT A/Z RATIOS IN SINGLE RADIO-FREQUENCY QUADRUPOLE(RFQ) CHANNEL

Vladislav Altsybeyev
Saint Petersburg University
Russia
v.altsybeev@spbu.ru

Yuri Svistunov
Saint Petersburg University
Russia,
JSC "NIIEFA"
Russia
svistunov@luts.niiefa.spb.su

Alexander Durkin
Saint Petersburg University
Russia
durkinap@mail.ru

Dmitry Ovsyannikov
Saint Petersburg University
Russia
d.a.ovsyannikov@spbu.ru

Article history:

Received 21.06.2018, Accepted 03.09.2018

Abstract

The preacceleration of multicharged ions with the different A/Z ratios extracted from electron cyclotron resonance (ECR) sources is discussed in this report. The capture ratio, emittances and current values of multicharged ions may be better if the ions are preaccelerated before their injection into a booster synchrotron. There is a considerable possibility of separate preacceleration of multicharged ions with different A/Z ratios in a single radio-frequency quadrupole (RFQ) channel. The magnitude of the injection energy into RFQ is about a few keV/u whereas the magnitudes of the injection energy into booster or following linac cascade are $\geq$300 keV/u. In addition in this paper we discuss the approach of the fast channel parameter optimization technique by using swarm computations and gradient descend for improving the capture ratio. The optimizations aimed at changing the regular part of the RFQ or matching section profile to improve the matching of the arbitrary oriented in phase space input beam.

Key words

RFQ accelerator, multicharged ion, linear accelerator, RFQ design, optimization.

1 Introduction

The purpose of this paper is to study the possibility to use a radio-frequency quadrupole (RFQ) with high operating frequency as a part of a multicharged ion beams compact injector to provide required beam characteristics before the injection of ions into a drift tube linac (DTL) or booster synchrotron. In general the main goal of RFQ design is to minimize emittance on its output. In this purpose it is useful to use a mathematical optimization methods to improve RFQ characteristics.

At present multicharged ions are used for different applications purposes such as implantation, medical radiation therapy, filter manufacturing and researches of nuclear structure. In this last case contemporary heavy ion injectors are complex systems which can include many different elements, for example (Martel, Acosta and et al., 2014): an ECR source, an extracting system, magnetic and electrostatic lenses, an accelerating column, single and multi–harmonic bunchers, a RFQ, superconducting resonators. In the papers (Angert, Dahl, Glatz and et al., 1991; Angert, Dahl, Glatz and et al., 1990) it has been shown that the use of RFQ after low-energy beam transport(LEBT) improves emittance, capture ratio and current value ot the ion beams.

Resonators for multicharged ion injector that could accelerate the ions in diapason from hydrogen to uranium and from carbon to uranium were considered in papers (Zhao, Andreev, Doleans and et al., 2004) and (Andreev, Alexeev, Balabin, Karts and

Metreveli, 2014) respectively. Naturally, the operating frequencies of these resonators are low (85 and 5 MHz accordingly), and they need a strong additional focusing magnetic field to provide good particle dynamics. But such multipurpose program is nor always necessary.

The use of single accelerator for the preacceleration of two or more ion types provides a cheaper and more compact preaccelerating part of the big accelerating system that produce isotopes of 1-2 MeV/u energy. The successful acceleration of the different types of ions separately in single RFQ channel depends on the fulfillment of a few conditions.

1. Initially RFQ channel is designed to accelerate an ion beam with the greatest A/Z ratio. It is the main particle.
2. Velocities of the ions of different types injected into the RFQ channel must be equal to the RFQ input.
3. To obtain better conditions for the acceleration of other ions (not main) the matching section geometry needs to be optimized (see (Ovsyannikov, Durkin, Ovsyannikov and Svistunov, 2016)) and there should be a possibility to change the intervane voltage depending on the ion type in the determined limits.

In this paper we consider only separate acceleration of different types of ions.

The examples of the proposed modeling system and description of the used codes are given below. The initial data for modeling can be found in (Schlitt and Ratzinger, 1998; Minaev, Ratzinger and Schlitt, 1999; Angert et al., 1991; Angert et al., 1990; Gikal, 2013).

The optimization of the beam characteristics on injector output depends on the optimization of separate parts of an injector; however, to achieve this mathematical control theory is not always suitable. It is rather difficult, for example, for the cases of an ECR source or a stripper.

A simple case is the separate acceleration of the beams $H^{\pm}$ and $D^{\pm}$ in single accelerating RFQ channel, which includes a plasma source (milticasp or magnetron type) with hydrogen or deuterium working gas, electrostatic LEBT with electromagnetic correctors, RFQ and DTL.

A possible procedure for dynamics optimization in LEBT has been described in the paper (Kozynchenko and Svistunov, 2006). In addition, a possible optimization procedure of dynamics in the RFQ for a mismatched beam is described in ref. (Ovsyannikov, Ovsyannikov and Chung, 2009*a*), and in ref. (Ovsyannikov et al., 2016), this procedure was generalized for separate acceleration of two beams.

In the case of separate acceleration of $H^{\pm}$ and $D^{\pm}$ ions from a single source with uses two working gases (hydrogen and deuterium), an electrostatic LEBT has enough control parameters (number and poteltials of electrodes for lenses, channel diameter and so on) to obtain the approximate values of $H^{\pm}$ and $D^{\pm}$ emittances at the RFQ entrance. In the general case, an experimental and a modeling efforts can be proposed and their effects may be analyzed to achieve the required results.

2 RFQ optimization and beam dynamics simulations

2.1 Main idea and equations

In our previous work (Ovsyannikov, Ovsyannikov, Altsybeyev, Durkin and Papkovich, 2014), we proposed the design of 47.2 MHz RFQ for the acceleration of heavy ions (A/Z=20). The optimization of the longitudinal motion of particles for this accelerator was performed using the (Beam dynamics optimization – radio-frequency quadrupole) BDO-RFQ code developed at the Saint-Petersburg State University. The BDO-RFQ code uses a traveling wave approximation of the accelerating field and the gradient descent optimization paradigm for the evaluation of synchronous phase sequence and acceleration efficiency. This approach required analytical representation of some minimized fitness functions.

In this work we use the Design of Accelerators, optImizations and SImulations (DAISI) code for designing the RFQs. For dynamics modeling of the RFQ, the DAISI uses the standard model with a standing-wave approximation (Ovsyannikov et al., 2014; Ovsyannikov et al., 2009*a*; Ovsyannikov, Ovsyannikov, Vorogushin, Svistunov and Durkin, 2006; Ovsyannikov, Ovsyannikov, Antropov and Kozynchenko, 2005)

$$\frac{d^2z}{d\tau^2} = 2\frac{qUT}{W_0 L}\cos(Kz)\cos(\omega\tau/c+\varphi_0),$$
$$\frac{dS_{11}^{x,y}}{d\tau} = S_{21}^{x,y},\ \frac{dS_{21}^{x,y}}{d\tau} = Q_{x,y}S_{11}^{x,y} + S_{22}^{x,y},$$
$$\frac{dS_{22}^{x,y}}{d\tau} = 2Q_{x,y}S_{12}^{x,y},$$
$$Q_x = \left(\frac{qUk}{W_0 a^2} + \frac{\pi UT}{W_0 L^2}\sin(Kz)\right)\cos(\omega\tau/c+\varphi_0),$$
$$Q_y = \left(-\frac{qUk}{W_0 a^2} + \frac{\pi UT}{W_0 L^2}\sin(Kz)\right)\cos(\omega\tau/c+\varphi_0).$$

Here c is the light speed, $\tau = ct$, ω is the angular frequency, L is the cell length, a is the minimal channel radius, U is the intervene voltage, T is the acceleration efficiency, W_0 is the particle rest energy, q is the particle charge, $K = \pi/L$, $k = 1 - 4T/\pi$, φ_0 is the initial phase, the six variables $S_{11}^{x,y}, S_{21}^{x,y}, S_{22}^{x,y}$ are the elements of the matrixes $G^{x,y} = \begin{pmatrix} S_{11}^{x,y} & S_{21}^{x,y} \\ S_{21}^{x,y} & S_{22}^{x,y} \end{pmatrix}$, which describes the dynamics of the initial transversal

distribution ellipses $G_0^{x,y}$ in the phase planes $(y, dy/dt)$ and $(x, dx/dt)$. Space-charge effects may also be included in this simple models on the optimization stage. However, in our optimization problem, we considered this effect only in the further simulation stages.

To solve the accelerator optimization problem we need to obtain a large set of channel parameters — lengths and modulations of cells except for the preselected intervane voltage and average channel radius. By using some smooth approximations of the dependences of the synchronous phases and the modulations on the cell number allows us to considerably reduce the number of the evaluated parameters (down to 10–20). In this case, the evolutionary optimization algorithms allow us to obtain good solutions within a reasonable time (dozen of minutes on modern shared-memory computers).

2.2 Particle Swarm Optimization

The DAISI uses an combination of evolutionary optimization algorithm (particle swarm method (Kennedy, 1995)) and gradient descent optimization with the numerical gradient calculation. These methods does not require any analytical calculations, but it is fast enough. Later, a set of modifications were made to the particle swarm method, but the classical approach works properly in our case.

The particle swarm method optimizes a problem by iteratively trying to improve a set of problem parameters with regard to a given fitness function (Kennedy, 1995; Tanweer, Auditya, Suresh, N. and N., 2016). It is a good choice for complex optimization problems because of its realization is simple and effective.

The general problem statement of the multi-variable function optimization can be represented in the following way:

$$F(\mathbf{x}) \to \min_{\mathbf{x} \in \mathrm{U}}.$$

Here F is the fitness function, $\mathbf{x}$ is the vector of the fitness function arguments, U is the set of allowable $\mathbf{x}$ values (search-space).

Following the original procedure of the particle swarm method, we have to create a set of algorithm agents called "particles", which move in the search-space U. Each algorithm agent with the number i at the t^{th} method iteration have the position $\mathbf{x}_i(t) \in U$. Therefore, the positions of the agent are associated with the fitness function arguments (optimized parameters).

The agents must move in the search-space U. Therefore, we have to associate the position increment $d\mathbf{x}_i(t)$ with the agent with the number i at the t^{th} method iteration.

The main particle swarm algorithm stages are described below (also see the flow chart in Fig. 1).

1. Agents initialization. The initial positions $\mathbf{x}_i(0),\ i = \overline{1, \ldots, N_a}$ (here N_a is the total number of agents) of the algorithm agents in the search-space U are assumed to be random (for example, using the uniform or the normal distribution). The initial positions increments $d\mathbf{x}_i(0),\ i = \overline{1, \ldots, N_a}$ may be zero.
2. Start of the new t^{th} algorithm iteration.
3. Calculation values of the fitness function $F_i(t) = F(\mathbf{x}_i(t)),\ i = \overline{1, \ldots, N_a}$ for each agent.
4. Calculation the best position $\mathbf{p}_i(t)$ for each agent using the following approach: $\mathbf{p}_i(t) = \mathbf{x}_i(k_0),\ k_0 = \operatorname{argmin}_{k \in [1,t]} F_i(k)$.
5. Calculation the best position $\mathbf{g}(t)$ for the the whole swarm using the following approach: $\mathbf{g}(t) = \operatorname{argmin}_{\mathbf{p}_i(t),\, i \in [1, N_a]} F(\mathbf{p}_i(t))$.
6. Check the convergence criteria. If the required solution accuracy achieved, the iterations stop.
7. Updating agents positions. It is possible to use the following equation to update the agents positions at the each method iteration:

$$\mathbf{x}_i(t+1) = \mathbf{x}_i(t) + d\mathbf{x}_i(t).$$

8. Updating agents positions increments. The agents positions increments are updated using the following equation

$$d\mathbf{x}_i(t+1) = d\mathbf{x}_i(t) + \varphi_p r_p(\mathbf{p}_i(t) - \mathbf{x}_i(t)) + \\ + \varphi_g r_g(\mathbf{g}(t) - \mathbf{x}_i(t)).$$

   Here φ_g and φ_p are the predefined weight parameters, $r_p \in [0, 1]$ and $r_g \in [0, 1]$ are random numbers.
9. Go to the step 2.

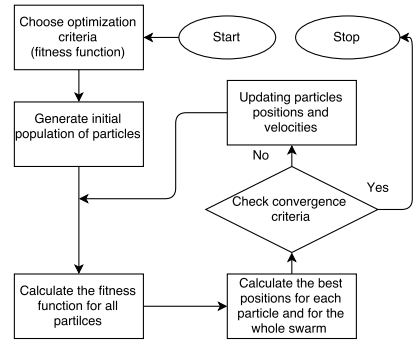

Figure 1. Particle swarm optimization flow chart

2.3 Gradient Descent Optimization

After the particle swarm method workflow is done, it is possible to some improve the obtained solution using the gradient descend optimization because of using only the particle swarm method does not guarantee achievement of the local fitness function minimum, but it can provide a good initial approximation of the solution. Therefore the combination of the particle swarm and the gradient descent methods will always work better than each of them separately.

In some cases it is possible to obtain the analytical representation of the fitness-function gradient (see refs. (Ovsyannikov et al., 2005), (Ovsyannikov, Ovsyannikov and Chung, 2009*b*), (Ovsyannikov et al., 2006)). But the calculation of gradient numerically using the finite-difference significantly easier and works reasonably well in the most cases. DAISI uses the numerical calculation of the gradient and the "heavy ball" modification of the gradient descent approach which can improve method convergence.

Therefore, the i^{th} component x_i^k of solution $\mathbf{x}^{k-1}$ on k^{th} algorithm iteration are updated using the following equation

$$x_i^k = x_i^{k-1} + \alpha^k \frac{F(\mathbf{x}^{k-1} + \Delta x_i^{k-1}) - F(\mathbf{x}_i^{k-1})}{\Delta x_i^{k-1}} + \\ + \beta(\mathbf{x}^{k-1} - \mathbf{x}^{k-2}).$$

Here α^k is the step on the k^{th} iteration, Δx_i^{k-1} is the small argument increment, β is the predefined constant.

2.4 RFQ Optimization Algorithm

Follow our approach the optimization of RFQ channel may be performed in several stages (see Fig. 2). At the first stage only longitudinal dynamics in the regular part of accelerator may be considered. After that if the input beam mismatches with the RFQ channel, it is possible to considerably improve the beam capture ratio using the modification of the matching section geometry profile. In addition, we can provide the minimization of the beam emittance growth. One can find more detailed description of these optimization stages below.

2.5 Procedure for Improving Capture Ratio

The RFQ design approach realized in the DAISI code is based on the division of the regular part of the RFQ channel in four parts — two parts for the gentle buncher, forming section and accelerating section. On each part with label k, the modulations and the synchronous phases are approximated using the following approach.

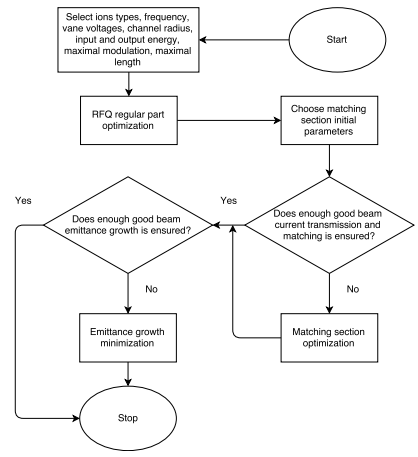

Figure 2. Flow chart of RFQ optimization algorithm

$$\varphi_i = \varphi_k + \frac{\varphi_{k+1} - \varphi_k}{N_k^{p_k}}(i - \sum_{j=0}^{k} N_j)^{p_k},$$

$$m_i = m_k + \frac{m_{k+1} - m_k}{N_k^{q_k}}(i - \sum_{j=0}^{k} N_j)^{q_k}.$$

Here i is the cell number, φ_k and m_k are synchronous phase and modulation at the beginning of the part with the label k, q_k and p_k are non-negative constants, N_j is the number of cells that forms a part with the label j. In the first part we assume $m_0 = 1$ and $\varphi_0 = -\pi/2$. The matching section is located before the regular part of the RFQ channel. Therefore, we have to obtain a set of 18 parameters N_k, q_k, p_k, φ_{k+1}, m_{k+1}, $(k = \overline{0...3})$, which will determine the geometry of RFQ electrodes.

The following expression determines the part of the non-accelerated particles that is used as a fitness function for improving the capture ratio.

$$F_1 = \sum_{\alpha=1}^{\alpha=N_\alpha} \sum_{k=1}^{N_p} f_1(W_{\alpha_k}),$$

$$f_1(W_{\alpha_k}) = \begin{cases} 1, & if \ \left|\frac{W_{\alpha_k} - W_\alpha}{W_\alpha}\right| > \Delta W_{\lim}, \\ 0, & else. \end{cases}$$

Here N_α is the number of accelerated ion types, N_p is the number of macroparticles, W_α is the average output energy of an ion beam with label α, W_{α_k} is the output macroparticle energy and $\Delta W_{\lim}$ is a constant. In this stage, we obtain modulations and synchronous phases of each cells.

One of the possible matching section optimization procedures is described in (Ovsyannikov et al., 2009*b*). However, in the present work, we propose a new procedure. As a starting point for optimization, use

the quadratic matching section profile. In this case the matching section radius r_i is approximated using the following expression.

$$r_i = r_m + \frac{r_c - r_m}{N_m^2} i^2.$$

Here, i is the cell number, r_c is the average radius of the channel regular part, r_m is the matcher maximal radius and N_m is the number of cells in the matcher. The matching section radius r_i is optimized in this procedure by using the following fitness function for improving the transmission rate.

$$F_2 = \sum_{\alpha=1}^{\alpha=N_\alpha} \sum_{k=1}^{N_p} f_2(S_{11}^{x,y}(z)),$$

$$f_2(S_{11}^{x,y}(z)) = \begin{cases} 1, & if \ \exists z: \ S_{11}^{x,y}(z) > c_a a(z), \\ 0, & else. \end{cases}$$

We recommend to choose a constant c_a in the $(0.5,\ 0.8)$ range. In other words when using a simple beam dynamics model, we have to ensure the transmission of the beam through a channel with a sufficient margin.

2.6 Emittance Growth Minimization Procedure

Additionally, we can minimize the beam emittance growth. The following expression that determines the level of the overlapping of the output ellipses is used as a fitness function in this optimization stage (Ovsyannikov et al., 2016).

$$F_2 = \sum_{\alpha=1}^{\alpha=N_\alpha} \sum_{k=1}^{N_p} \left[\left(\frac{1}{N_p} \sum_{j=1}^{N_p} S_{21_{\alpha_j}}^x - S_{21_{\alpha_k}}^x \right)^2 + \right.$$
$$\left. + \left(\frac{1}{N_p} \sum_{j=1}^{N_p} S_{21_{\alpha_j}}^y - S_{21_{\alpha_k}}^y \right)^2 \right].$$

In this stage we can make a small correction in the modulations of the channel cells and obtain the matching section parameters.

2.7 Particle in Cell Simulations

For the accurate estimation of the beam characteristics, the electrode parameters calculated by the DAISI were exported to the LIDOS RFQ Designer code (Bondarev, Durkin, Ivanov and et al., 2001). Later, LIDOS was used for the final correction and selection of the channel parameters, considering the real shape of the electrodes, their possible sectioning for mechanical processing, electrodynamics settings, etc. Full 3D particle-in-cell simulations were performed by LIDOS considering the real shape of electrodes.

3 Examples of Preacceleration of Carbon Ions with Z=4+ and Z=6+

The preacceleration of C_{12}^{4+} and C_{12}^{6+} ions was considered in papers (Schlitt and Ratzinger, 1998; Minaev et al., 1999) with respect to the German proposal for the HIT medical facility. Because the yield of C_{12}^{6+} ions from ECR source is small, C_{12}^{4+} ions were accelerated up to 7 MeV/u by a tandem of RFQ + IH-linac and necessary quantity of C_{12}^{6+} ions was obtained by stripping of C_{12}^{4+} ions on special foil. It is possible in the future to obtain quite enough quantity of C_{12}^{6+} ions directly from ECR source and only then RFQ channel may be used for the acceleration of both C_{12}^{4+} and C_{12}^{6+} ion type.

The characteristics of the beam and the RFQ channel parameters are presented in Table 1 and plotted versus the cell number in Fig. 3. The initial data for modeling can be found in works (Schlitt and Ratzinger, 1998; Minaev et al., 1999). We suppose that C_{12}^{4+} ion beam may be optimally matched to the RFQ channel with the help of LEBT and RFQ matching section, as discussed in (Schlitt and Ratzinger, 1998). In this case, the beam of C_{12}^{6+} can be mismatched. To estimate a capture ratio of mismatched C_{12}^{6+} beam, the neutral input ellipses in XdX and YdY axes were used. Dependences of the current capture ratio on the input current are presented in Fig. 4. We have also analyzed the dependence of the main characteristics of accelerated C_{12}^{6+} ions on the intervane voltage. The main results are as follows: with the increase intervane voltage, capture ratio, bunch momentum width and output emittance are increase, while the bunch phase width decreases (see Fig. 5).

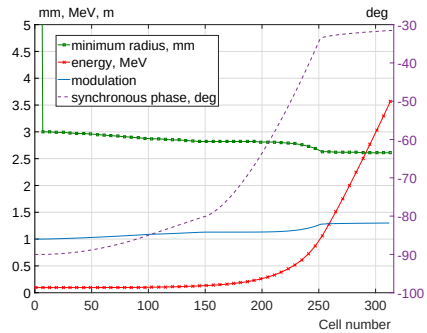

Figure 3. Carbon RFQ Design Parameters

4 Examples of Preacceleration of Hard Multicharged Ions Yb, Pb, Bi

The characteristics of the beam and the RFQ channel parameters are presented in Tables 2, 3. The initial data for modeling can be found in works (Angert et al., 1991; Angert et al., 1990). As in the previous examples, we suppose that the LEBT system, together with the source and RFQ matching section, provides

Input ions energy, MeV	0.096
Output ions energy, MeV	3.57
Operating frequency, MHz	216
Kilpatrick factor Emax/Ekilp	1.8
Intervane voltage for C_{12}^{4+} ions, kV	70
Intervane voltage for C_{12}^{6+} ions, kV	46.6
Average channel aperture radius, mm	3
Maximal modulation	1.3
Input impulse current, mA	0-10
Input emittance, pi·cm·mrad (RMS, norm)	0.03
Initial momentum spread, %	± 2.5
Accelerator length, m	1.83
Zero current 90% emittance growth (C_{12}^{4+})	2.1
Bunch phase width (90%, 1 mA, C_{12}^{4+}), deg	38
Bunch momentum width (90%, 1 mA, C_{12}^{4+}), %	2.3

Table 1. Main carbon RFQ parameters

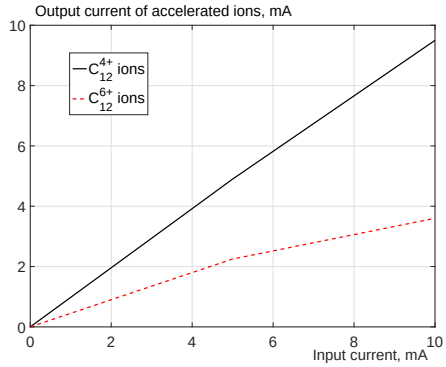

Figure 4. Dependence of the current of accelerated ions on the input impulse current

an optimum matching for the beam of Pb_{208}^{28+} to the RFQ channel. To estimate the capture ratio of the mismatched beams of $Bi\,^{35+}_{209}$ and Yb_{176}^{22+}, the neutral input ellipses in XdX and YdY axes were used. In addition we conduct a set of simulation for Yb_{176}^{22+} ions beam with different input emittance (Fig. 6). For each simulation the phase volume shapes changed with a change in the input emittance.

5 Examples of Preacceleration of Hard Multicharged Ions Kr, Ar

The characteristics of the beam and the RFQ channel parameters are presented in Tables 4, 5. The initial data

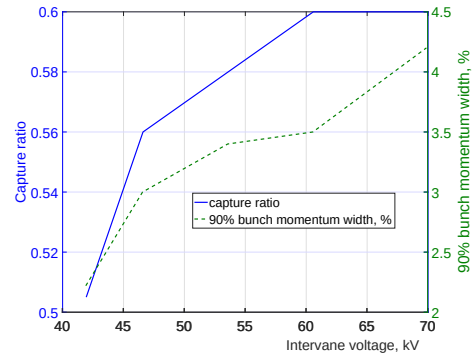

Figure 5. Dependences of the characteristics of accelerated C_{12}^{6+} ions for zero current on intervane voltage

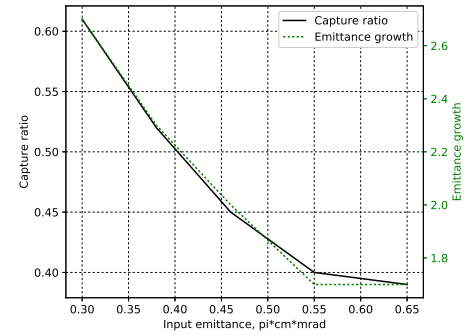

Figure 6. Dependences of some output characteristics of the accelerated Yb_{176}^{22+} ion beam on the input emittance

for modeling can be found in work (Gikal, 2013).

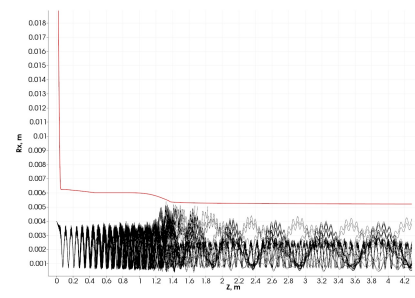

Figure 7. Trajectories of Ar_{40}^{8+} ion before optimization calculated using DAISI. Capture ratio in standing-wave model is 0.52

The system of the axial beam injection described in this work produces the beam of Kr_{86}^{13+} ions with 8 mm width and 35 mrad divergence. For matching this beam with the RFQ, the channel radius has to be increased to 6.25 mm. The capture ratio in this case considerably decreases to 0.4 obtained using the LIDOS and 0.52 obtained using the DAISI. It also should be noted that the capture ratio magnitude in the standing-wave

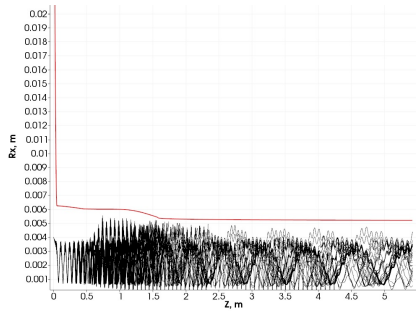

Figure 8. Trajectories of Ar_{40}^{8+} after gradient descend optimization calculated using DAISI. Capture ratio in standing-wave model is 0.78

Input ions energy, keV/u	3
Output ions energy, keV/u	350
Operating frequency, MHz	108
Intervane voltage for Kr_{86}^{13+} ions, kV	90
Intervane voltage for Ar_{40}^{8+} ions, kV	68
Average channel aperture radius, mm	6.25
Maximal modulation	1.5
Minimal channel radius, mm	5.44
Input impulse current, mA	<0.2
Input emittance, pi·cm·mrad (RMS, normalized) (Kr_{86}^{13+})	0.03
Input emittance, pi·cm·mrad (RMS, normalized) (Ar_{40}^{8+})	0.04
Initial momentum spread, %	±2.5
Accelerator length, m	4.66

Table 4. Main RFQ parameters for multicharged ions Kr, Ar

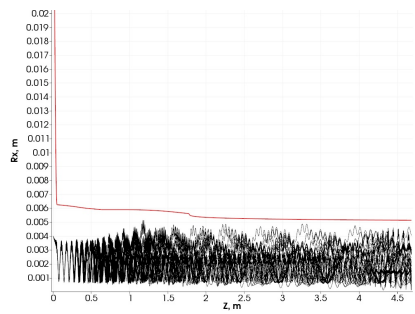

Figure 9. Trajectories of Ar_{40}^{8+} after proposed optimization approach (particle swarm + gradient descend) calculated using DAISI. Capture ratio in standing-wave model is 1.0

	Capture ratio	Bunch phase width (90%), deg	Bunch momentum width (90%), %	emittance growth (90%)
before optimization				
Kr_{86}^{13+}	0.4	22.2	1.28	2.4
Ar_{40}^{8+}	0.38	21	1.34	1.8
after optimization				
Kr_{86}^{13+}	0.59	21.6	1.26	2.3
Ar_{40}^{8+}	0.59	20.6	1.3	1.7

Table 5. Output parameters of Kr, Ar accelerated beams before and after optimization calculated using LIDOS

Input ions energy, keV/u	2.5
Output ions energy, keV/u	300
Operating frequency, MHz	108
Kilpatrick factor Emax/Ekilp	1.8
Intervane voltage for Pb_{208}^{28+} ions, kV	90
Intervane voltage for Yb_{176}^{22+} ions, kV	90
Intervane voltage for $Bi\,^{35+}_{209}$ ions, kV	72.3
Average channel aperture radius, mm	4.42
Maximal modulation	1.6
Minimal channel radius, mm	3.4
Input current, mA	<0.2
Input emittance, pi·cm·mrad (RMS, norm)	0.046
Initial momentum spread, %	±2.5
Accelerator length, m	3.43

Table 2. Main RFQ parameters for multicharged ions Yb, Pb and Bi

	Capture ratio	Bunch phase width (90%), deg	Bunch momentum width (90%), %	emittance growth (90%)
Pb_{208}^{28+}	0.85	24	1.5	1.6
Yb_{176}^{22+}	0.45	27.2	1.74	2.0
$Bi\,^{35+}_{209}$	0.45	24.6	1.8	1.9

Table 3. Output parameters of Yb, Pb and Bi accelerated beams

approximation (using the DAISI) is better than the

capture ratio magnitude obtained using the particle-in-cell simulations (using the LIDOS). The transversal trajectories of Ar_{40}^{8+} for this case are presented in Fig. 7. We performed comparison of the above described optimization approach and the simple gradient descend procedure. By using the gradient descend optimization the capture ratio was improved from 0.52 to 0.78 in the DAISI (Fig. 8). However, by using the above described optimization procedure, the capture ratio was improved from 0.52 to 1.0 in the DAISI (see Fig. 9). Therefore the application of the proposed approach of the combination of the particle swarm and the gradient descent methods results in better capture ratio than application both of them separately.

6 Conclusion

In some cases it is possible to organize preacceleration a few types of multicharged ions before injection into booster or DTL by using single chain of compact accelerators with high operating frequency. The RFQ placed after the LEBT is important part of the preacceleration tract. Modelling's results given above show that the geometrical optimization of the matching section and the regular part of the RFQ vanes by using the fast stochastic optimization methods allows to obtain good RFQ output beam parameters, thus allowing the further acceleration of the ions in a DTL or an IH resonators without using an additional strong magnetic field. Sometimes low capture ratio strong depends on the emittance on the RFQ input. The initial data used in this paper are published experimental and calculated data and this is not always best over in the world.

References

Andreev, V., Alexeev, N. N., Balabin, A., Karts, M. M. and Metreveli, A. A. (2014), Upgrade of heavy ion injector for ITEP-TWAC facility, *in* 'Proceedings of IPAC2014, Dresden, Germany ', pp. 3283–3285.

Angert, N., Dahl, L., Glatz, J. and et al. (1990), A New 1.4 MeV/U Injector Linac for the Unilac, *in* 'Proceedings of the Linear Accelerator Conference 1990, Albuquerque, New Mexico, USA', pp. 749–751.

Angert, N., Dahl, L., Glatz, J. and et al. (1991), Commissioning of the New Heavy Ion Injector at GSI, *in* 'Conference Record of 1991 IEEE Particle Accelerator Conference Part 5 (of 5)', pp. 2981–2983.

Bondarev, B., Durkin, A., Ivanov, Y. and et al. (2001), The LIDOS.RFQ.Designer development, *in* 'Particle Accelerator Conference', Vol. 4, pp. 2947–2949.

Gikal, B. N. (2013), The new generation of heavy ion cyclotrons for applied research and industrial applications, PhD thesis, Joint Institute for Nuclear Research, Dubna.

Kennedy, J. (1995), Particle swarm optimization, *in* 'Proceedings of IEEE International Conference on Neural Networks IV', pp. 1942–1948.

Kozynchenko, S. A. and Svistunov, Y. A. (2006), 'Application of field and dynamics code to LEBT optimization', *Nuclear Instruments and Methods in Physics Research Section A* **558**(1), 295–298.

Martel, I., Acosta, L. and et al., C. D. R. (2014), ECOS-LINCE: a high intensity multi-ion superconducting linac for nuclear structure and reactions, *in* 'Proceedings of IPAC2014, Dresden, Germany', pp. 3301–3303.

Minaev, S., Ratzinger, U. and Schlitt, B. (1999), APF or konus drift tube structures for medical synchrotron injectors – a comparision, *in* 'Proceedings of the 1999 Particle Accelerator Conference, New York', Vol. 4, pp. 3555–3557.

Ovsyannikov, A. D., Durkin, A. P., Ovsyannikov, D. A. and Svistunov, Y. A. (2016), 'Acceleration of different ion types in single RFQ structure', *Problems of Atomic Science and Technology* **3**(103), 54–56.

Ovsyannikov, A. D., Ovsyannikov, D. A., Altsybeyev, V. V., Durkin, A. P. and Papkovich, V. G. (2014), 'Application of optimization techniques for RFQ design', *Problems of Atomic Science and Technology* **3**(91), 116–119.

Ovsyannikov, A. D., Ovsyannikov, D. A. and Chung, S.-L. (2009*a*), 'Optimization of a radial matching section', *International Journal of Modern Physics A* **24**(5), 952–958.

Ovsyannikov, A. D., Ovsyannikov, D. A. and Chung, S.-L. (2009*b*), 'Optimization of Matching Section of an Accelerator with a Spatially Uniform Quadrupole Focusing', *Technical Physics. The Russian Journal off Applied Physics* **54**(11), 1663–1666.

Ovsyannikov, D. A., Ovsyannikov, A. D., Antropov, I. and Kozynchenko, V. (2005), BDO-RFQ code and optimization models, *in* 'Physics and Control, 2005', pp. 282–288.

Ovsyannikov, D. A., Ovsyannikov, A. D., Vorogushin, M. F., Svistunov, Y. A. and Durkin, A. P. (2006), 'Beam dynamics optimization: Models, methods and applications', *Nuclear Instruments and Methods in Physics Research, Section A: Accelerators, Spectrometers, Detectors and Associated Equipment Volume* **558**(1), 11–19.

Schlitt, B. and Ratzinger, U. (1998), Design of a carbon injector for a medical accelerator complex, *in* 'Proceedings of the EPAC-98', Vol. 4, pp. 2377–2379.

Tanweer, M. R., Auditya, R., Suresh, S., N., S. and N., S. (2016), 'Directionally Driven Self-Regulating Particle Swarm Optimization algorithm', *Swarm and Evolutionary Computation* **28**, 98–116.

Zhao, Q., Andreev, V., Doleans, M. and et al. (2004), Design improvement of the RIA 80.5 MHz RFQ, *in* 'Proceedings of LINAC 2004, Lubeck, Germany', pp. 599–601.